Flippy: A Soft, Autonomous Climber with Simple Sensing and Control

Melinda Malley[1], Michael Rubenstein[2], and Radhika Nagpal[1]

***Abstract*— Climbing robots have many potential applications including maintenance, monitoring, search and rescue, and self-assembly. While numerous climbing designs have been investigated, most are limited to stiff components. Flippy (Fig. 1) is a small, flipping biped robot with a soft, flexible body and on-board power and control. Due to its built-in compliance, flipping gait, and corkscrew gripper, it can autonomously climb up and down surfaces held at any angle relative to gravity and transition from one surface to another, without complex sensing or control. In this paper, we demonstrate the robot's ability to flip consistently over a flat Velcro surface and 2D Velcro track, where it reliably climbs vertically, upside down and back to a flat surface, completing all the interior transitions in-between.**

I. INTRODUCTION

Climbing robots have an exciting array of potential applications [1], including maintenance activities in and outside buildings, monitoring and inspection, and search and rescue. In addition, climbing robots that climb over one another can form the basis of self-assembling swarms, constructing emergency and temporary structures. In all of these cases, climbing robots provide access to spaces where it could be dangerous or difficult for humans to operate, whether at high altitudes, in fragile environments, or within cramped pipes.

While potentially very useful, climbing robots also present major design challenges for locomotion and attachment. A robot inspecting building interiors, for example, must be able to climb vertically, over ceilings, return down to the ground, and transition between all of those planes. To do this, a climbing robot must attach strongly to the surface and support its own body weight in any orientation, but still be able to detach easily to continue to move. While animals achieve this in many elegant forms, climbing robots have yet to reach similar capacities. Most climbing robots have focused on vertical climbing or climbing ramps of increasing steepness [2], [3], [4], [5], [6], [7], [8]. Some are also able to transition between surfaces [9], climb upside down, or both [10], [11]. One tank-like robot [12] has shown impressive capabilities, including internal and external transitions and climbing over obstacles, but is unable to move from vertical walls to the ceiling. Biped robots such as RAMR1[13] and W-Climbot[14], from which our robot takes inspiration, are able to climb at many angles and transition between all interior angles, yet they require either human tele-operation or complex path planning, and remain tethered due to the high energy required by their suction adhesion mechanism.

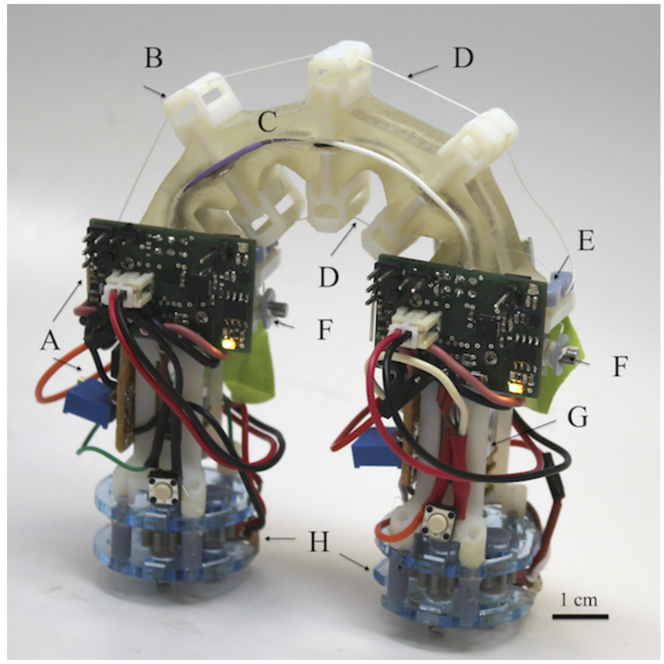

Fig. 1. Flippy robot. A) Printed circuit board and additional board for IR sensor circuit B) Stiff body part C) Flexible body part with embedded wire to connect between boards D) Cable E) Tension sensor: a pin joint link which pushes a switch on the PCB when the cable is in tension F) Winding spool and motor G) Gripper motor H) Corkscrew gripper with housing

Thus far, almost all climbing robots have been limited to rigid materials and components, often adding joints to allow transitions from one surface to another. One exception is the Treebot [15], another biped which uses springs for compliance. Meanwhile, climbers in nature display much more flexibility. Larger climbers like squirrels have a skeleton structure, but are still made of soft tissues, and many insects such as caterpillars, slugs, and inchworms are completely soft and compliant.

Inspired by these soft climbers, we designed Flippy, a small biped robot with a soft, flexible body and grippers on each end. While the current prototype is limited to 2D Velcro surfaces, Flippy demonstrates the potential of soft bodied climbers. The robot is equipped with only limited sensing and a simple control algorithm, but thanks to its compliant body and flipping gait, Flippy is able to autonomously climb up and down surfaces held at any angles relative to gravity, including vertically and upside down, and can transition between interior planes in different orientations.

*This work was supported and funded by the Wyss Institute

[1]School of Engineering and Applied Sciences, Wyss Institute for Biologically Inspired Engineering, Harvard University `melindamalley@fas.harvard.edu`

[2]Electrical Engineering and Computer Science Department, Mechanical Engineering Department, McCormick School of Engineering, Northwestern University `rubenstein@northwestern.edu`

II. ROBOT DESIGN

The Flippy robot, shown in Fig. 1, is a small biped robot which utilizes a flexible body and flipping gait to climb and transition between surfaces. The body is modeled after shape deposit manufacturing finger designs used for robotic hands and graspers [16], [17]; cables drawn through stiff sections of the body exert a torque and cause the flexible portions of the body to bend. In the Flippy robot, motors control cable lengths on both the top and bottom to allow for the flipping motion. Grippers attached at both ends consist of corkscrews which wind into and out of Velcro loops to attach to surfaces at any orientation.

A. Locomotion and Body Design

Though flipping mostly calls to mind human gymnasts, a few animals also use similar gaits: some spiders, caterpillars and other animals use wheel like motions to escape predators [18], and the adult stromatopod Nannosquilla decemspinosa flips its body when stuck out of water [19]. Flipping has a few drawbacks: it requires a stronger gripper to counterbalance the moment of the extended body length, and it is relatively slow. However, flipping can be very useful: it allows robots to easily transition between surfaces at different angles, as demonstrated by two previous biped robots [13], [14]. Similarly, many re-configurable robots such as the M-blocks [20] use the pivoting cube model, which operates on a similar principle. This indicates that flipping may be a useful gait in self-assembly as well as climbing.

In the Flippy robot, flipping eliminates the need for any sort of complex control. The gait essentially acts as a search pattern for the closest available surface, as shown in Fig. 2. Once the robot finds a surface, the flexible body allows the robot gripper to conform to the surface angle without the use of a human operator or complex control system. In almost all x-y positions, the gripper has multiple possible orientations, due to the compliance of the flexible segments. Although we model the flexible joints as simple bending joints, each section also has about $\pm$ 3 mm of possible translation, and of course can bend anywhere along the flexible section, allowing even more possible contact orientations.

To design the locomotion of the robot, we created a simple, geometric model. For simplicity, we ignored the viscoelastic behavior of the flexible material and assumed negligible friction i.e. the cable will shorten equally in all segments. In the physical robot, curved flexible segments (seen in Fig 3) encourage centered bending, to keep it consistent with the model. Using these assumptions, we first reduced the scope of the model to one segment only, used this to inform the design of the robot, and then modeled the flipping gait.

Geometric Model

A close up of one segment is shown in Fig. 3. Here w_f is the width at the center of the flexible component, c_b the bottom cable length, c_t the top cable length, h_s the height of the stiff component from the cable to the center. The bending angle $theta$ is the angle between the two stiff segments. In Fig. 3, when the robot is not bending, and the stiff segments are parallel, this is simply zero. w_f will become an arc length as the flexible segment bends, but we assume the magnitude of the length will remain constant (no elongation or compression). Maximum bending will occur when the two stiff components collide. Thus the maximum angle in radians is simply

$$\theta_{max} = w_f / h_s \tag{1}$$

which we can use to determine h_s and w_f. To navigate flat surfaces, the robot must bend at least 180° from its unbent position, both shown in Fig. 2. Climbing vertical walls requires an extra safety factor, as the robot may tilt away from the wall. Adding segments increases the length of the robot, but reduces bending in the cables and therefore cable friction. The final robot consists of four flexible segments with a θ_{max} of 57° for a total of 228° of bending.

Treating h_s and w_f as constants, we determined the dependence of θ on the length of the bottom cable c_b, as well as the relation between the change in lengths of c_b and the top cable c_t or $\Delta c_b / \Delta c_t$, which determines the relative winding and unwinding speeds of the motors while flipping.

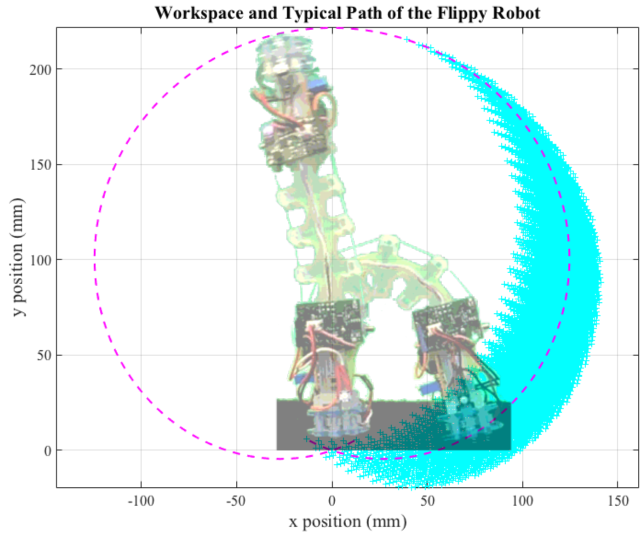

Fig. 2. Flipping trajectory of the robot. The dotted line shows a typical flip, assuming equal bending in all sections. The blue markers show the workspace of the robot.

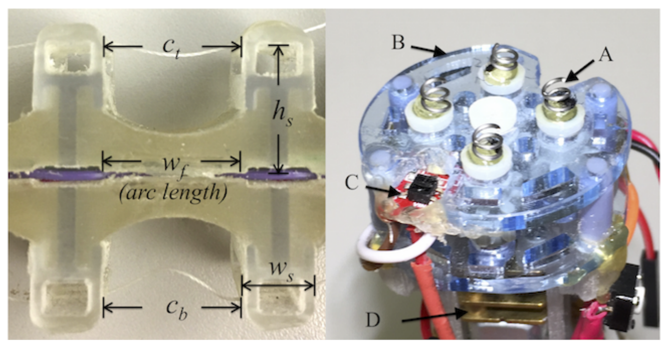

Fig. 3. Left: Close up of a body segment. The flexible segment is concave to encourage bending at the middle. Right: Close up of corkscrew gripper: A) Corkscrews mounted on Lego gears B) Acrylic housing C) IR reflectance sensor D) Gripper motor

Using basic trigonometry, we find

$$c_b = 2(w_f/\theta - h_s)\sin(\theta/2) \tag{2}$$

and

$$c_t/c_b = \frac{w_f/\theta + h_s}{w_f/\theta - h_s} \tag{3}.$$

Using Matlab, we solved c_t numerically for a sample of lengths c_b. The results were plotted and linearized via the polyfit function to find $\Delta c_b/\Delta c_t$. The process was repeated for several values of h_s and w_f, giving us a range of values for $\Delta c_b/\Delta c_t$ from about -0.87 to -0.95. Winding the cable at these speed ratios would allow us to perform half a flip, from a neutral (unbent robot) to $180°$ as shown by the background robot in Fig. 2. The first half of the flip, $-180°$ to neutral, can be accomplished by treating the winding motor as the top cable and inverting the speed ratio. However, for simplicity and to prevent tangling of the cables, we decided to implement a sensor feedback system using the tension switches in Fig. 1E. For most of a flip, the unwinding motor moves whenever the robot senses tension in the cable, when the cable pushes a lever into a mechanical switch. At the beginning of a flip, to ensure that cables were not overtightened, the unwinding cable was run at a constant speed, at a speed ratio slightly above that of the model.

The final dimensions of the robot were chosen as follows: h_s is 15.2 mm, the minimum height to accommodate the motors. From (1), w_f is also 15.2 mm. The thickness of the flexible components was chosen experimentally as the minimum thickness capable of supporting its own moment arm, (i.e. the robot body remained straight when held at one end perpendicular to gravity). The width of the stiff components, w_s in Fig. 3, was kept small in order to minimize the moment arm of the robot, but allow for space between the two grippers, without which the robot would not be able to bend more than $180°$.

Using the chosen dimensions and assuming centered bending, the robot was modeled as a four joint manipulator to calculate the trajectory shown in Fig. 2. The center of the flexible segments were treated as revolute joints. The Denavit-Hartenberg convention was used to calculate the position of the moving gripper relative to the attached gripper. The dotted line of Fig. 2 shows the trajectory of the robot, assuming that the cable length is the same in all segments. The blue markers show the workspace, removing this assumption and sampling $5°$increments of each angle. In reality, the workspace is slightly smaller as the current spacing of the grippers reduces the possible bending to $210°$ rather than $228°$. In addition, due to friction, the cable in sections closer to the motor will shorten more quickly than in the farther sections, giving us a slightly different typical trajectory than the one modeled. To account for this, we chose for the winding motor to always be on the attached gripper. This will cause the robot to reach past the predicted trajectory in the forward direction, giving us an advantage in vertical climbing, though possibly a disadvantage in some transitions.

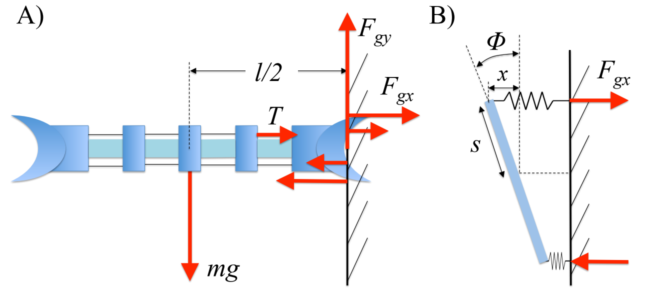

Fig. 4. a) Free body diagram of the robot vertical climbing in its extended position. The motor winding the cable must balance the moment arm of the robot as well as the resistance to bending of the flexible joints. Similarly the gripper must be able to hold the moment arm of the robot. b) Model of the corkscrew gripper as spring point forces

Motor Selection

Pololu Micro Metal Gearmotors were chosen for their small size, price, and variety of speed and torque capacities. The necessary motor torque capacity was calculated by considering the worst case scenario: vertical climbing with the robot fully extended (Fig. 4). Here, the motor torque is the sum of the torque required to bend the flexible components and the moment arm of the robot. The bending torque was found experimentally by hanging weights from the control cable until the robot was bent $180°$ and multiplying this force by the combined radius of the motor shaft and cable spool r_m. The torque applied by the moment arm of the robot is simply $mgl/2$. This was approximated as 0.1 Nm, for a 200 mm long, 100 g robot. Since the tension is applied at $h_s/2$ from the combined radius of the motor shaft and spool, the moment arm was multiplied by r_m/h_s. To account for additional forces, changes to the robot mass and length, and additional bending resistance at angles greater than $180°$, the sum of these two moments was multiplied by a safety factor of 3, and a motor with this torque capacity selected.

B. Gripper Design

Attachment is one of the critical design questions for climbing robots. Many different mechanisms have been developed, including magnets [11], [21]; electroadhesion [4], [3]; wet and dry adhesion [7], [6], [2]; needles, hooks and micro-spines [8], [22], [9], [15]; and pinchers and more traditional manipulators[5], [23]. Many of these, such as electroadhesion and most adhesives, are designed to work well with robots that sit close to the wall; they are strong in sheer but weak in peel. These would require significant modification to be applicable to our robot due to its flipping gait which applies a large moment to the gripper. Two of the climbing bipeds [13], [14] which inspired our robot use active suction. This allows attachment to different surfaces types and supports the required torque but requires high power consumption and is almost always tethered. The other biped, Treebot [15], uses a pincher gripper with needle tips. This is closer to our design, and works well for tree trunks and branches, but would likely struggle with flat surfaces.

We prototyped and tested a number of gripping mechanisms before choosing the novel corkscrew gripper shown in Fig. 3, which screws and unscrews into Velcro loops. The main design criteria we considered were force and torque capacity, reliability, and energy consumption. Though the use of Velcro loops limits our choice of surfaces, it allowed us to test the flexible body and flipping gait with autonomous control. In the future, we envision using this mechanism to attach to Velcro covered robots to perform self-assembly. The corkscrew grippers could be exchanged, for example with a magnetic or pincher based gripper, for other applications.

In the corkscrew gripper, four small springs are treated as mini-corkscrews; each is connected to a central gear and motor which drives them forward and backward. Since the gripper must be able to resist the moment of the extended robot, multiple corkscrews placed at a small distance from the center of the gripper are more effective than a larger, central corkscrew. The square, four corkscrew configuration was chosen for ease of use with Lego 8 teeth plastic gears, a readily available, compact, and inexpensive way to connect the corkscrews to a central motor. The four corkscrew configuration was also advantageous due to its small footprint and ease of integration with the gripper touch sensors. Future robots designed for higher payloads might incorporate a larger gripper with more corkscrews.

The necessary attachment force for our gripper was determined using the worst case scenario of vertical climbing with the robot body fully extended (Fig. 4a). The gripper must provide large enough attachment forces to balance the moment of the robot (approximately 0.1 Nm) and deflect no more than 10°. To determine the desired dimensions of the corkscrews (the diameter of the coil and wire, number of turns on the cut springs), we modeled the gripper corkscrews as spring contact forces, assuming no breaking in the Velcro loops once attached. The model is shown in Fig. 4b, where ϕ is the angle of deflection, x is the change in length of the spring and F_x is the spring force. Since the robot is mostly symmetric, we ignored twisting and considered the robot in 2D, thus the distance s from the center of the gripper to the corkscrew, is the y component only. Given Hooke's law and using small angle approximations, we find that the torque exerted by the gripper is:

$$\tau = \sum ks^2\phi \tag{4}$$

where k is the spring constant

$$k = \frac{Gd^4}{8nD^3}, \tag{5}$$

G is the shear modulus of the material, d is the wire diameter, n is the number of coils and D is the diameter of the coil (defined as the outside diameter of the coil minus d). Using 10° as the maximum deflection angle ϕ for the torque applied by an extended robot, we found a range of appropriate wire and coil diameter combinations, and, considering size and other design constraints, chose from commercially available springs. Since k increases as the number of active coils decreases, we tested springs with varying n and chose the minimum which would still allow us a tight attachment to the Velcro, in this case, n=1.5. Lower n was also found experimentally to ease attachment and detachment. The pitch of the springs was determined experimentally to be approximately 1 mm based on ease of attachment and detachment in Velcro. As no commercially available springs had such a large pitch, the springs were plastically deformed by hand until the pitch was the correct length.

C. Sensors and Electronics

The robot is controlled from two custom printed circuit boards in a master-slave configuration, each with an ATmega328P microcontroller. The boards are identical except for an on/standby switch on the master board. Each board controls two motor outputs: one that controls the length of the bending cable and one that controls the corkscrew gripper. Both are also equipped with an RGB LED and serial output for debugging. Inputs to each board include a three axes accelerometer, a magnetometer, and the mechanical switch used to sense cable tension. An IR reflectance sensor (Pololu QTR-1A) acts as a binary touch sensor for the gripper, connecting to a comparator circuit and then into a digital input on the board. There are also connections for a flex sensor such as Sparkfun SEN-10264, which could be used in future versions of the robot. The run time for the robot while flipping is approximately 50 minutes to an hour, using two 150 mAh batteries (one per circuit board).

D. Fabrication and Specifications

The body of the robot is 3D printed in VeraClear and TangoPlus from Stratasys for ease of prototyping. Since the 3D printed flexible materials are susceptible to fatigue and aging, leading to cracks, a final version of the robot could be molded or partially molded with a silicone rubber. The PCBs are attached to the front side of each end of the robot with the batteries on opposite side to balance the weight distribution. The pin joint and lever for the tension switch are 3D printed and press fit into a corresponding hole on the body. Size 69 Nylon thread is used as the cable, which is threaded through the stiff components and attached to a printed cable spool. To manufacture the gripper, springs (McMaster 9663K52) were cut to length and connected via custom printed parts and epoxy into the gear train, which is sandwiched between two pieces of lasercut acrylic. Additional printed parts connect the train to the gripper motor (another Pololu Micro Metal Gearmotor), and the gripper to the body of the robot.

The final weight of the robot is 120.64 g. The body accounts for approximately one third of the weight (38 g), and the motors another third (9.4 g each). The grippers are approximately 6 g each. Batteries (4.5 g ea) and electronics account for the rest of the weight. The length of the robot is 235 mm from the tips of the corkscrews, giving the robot a total moment of 0.139 Nm (slightly larger than our approximation, but easily within the safety factor). The length of the bending portion accounts for less than half of the length (97 mm), while the motor housing and grippers

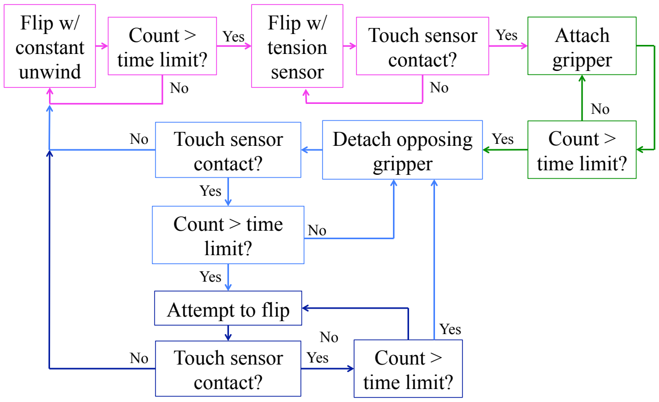

Fig. 5. Flow Diagram for Control 1 (first simple control algorithm). Each color represents a different state.

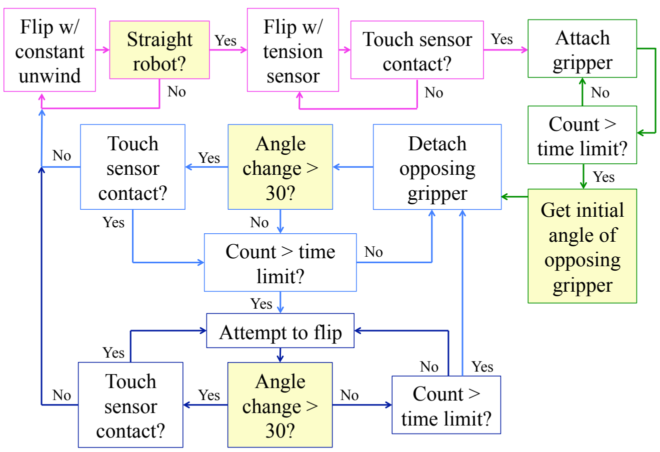

Fig. 6. Flow Diagram for Control 2 (control algorithm with IMU sensing). Changes from Control 1 are highlighted.

account for the rest. Future renditions of the robot could reduce the moment arm by changing the position of the motors and moving to a smaller gearbox.

E. Autonomous Control

Many climbing robots have focused on only attachment and locomotion, assuming applications where a climbing robot can remain tethered or even be tele-operated. Untethered robots, however, will make it easier to navigate complex spaces. In addition, swarms of climbers can be useful for many applications, such as search and rescue and our eventual goal of self-assembly, all of which will be difficult to impossible to implement without autonomous control. Using only two basic sensor inputs, the IMU and binary touch sensor, the Flippy robot is able to execute autonomous flipping, climbing, and transitioning.

We tested the Flippy robot using two control algorithms. Both consist of a simple state machine with the following states: flipping, attaching, and detaching of each side. The RGB LED indicated the current state of the robot as well as critical checks within each states.

The simpler control algorithm, or Control 1, uses only the binary touch sensor and is shown in Fig. 5. The robot starts in the flipping state, with one gripper attached and one free to move. It begins its flip by winding one cable in the forward direction, and simultaneously unwinding the opposing cable at a constant speed for a set time period. As mentioned previously, this unwinding period is useful in the case that during the detachment period the robot became twisted or bent in unexpected ways due to over-tightening of the cables. Once this period is over, the robot continues to flip, using its default method of unwinding only when it detects tension in the unwinding cable. As soon as the touch sensor detects a new surface, the robot switches to the attaching state, which merely runs the corkscrews forward (in the attaching direction) for a set period (about three seconds). It then switches to the detaching state for the opposing gripper. Here the robot runs the corkscrews backwards for a set period of time, and then tries to flip. As soon as the touch sensor no longer detects the surface, the robot will return to the flipping state.

As we show in the next section, Control 1 is sufficient for basic flipping and climbing. The second control method (Control 2) shown in Fig. 6, is similar to Control 1, but uses additional sensing to achieve higher reliability when transitioning between planes. One common issue with Control 1 was that during transitions the robot would reattach to the surface before completing the entire flip. To prevent this we used the IMU as a bend sensor and implemented a check to ensure that the robot passes through the neutral, extended straight position before it attempts to attach the moving gripper. Neutral here is found by calculating the orientation in the X-Y plane of each IMU and taking the absolute value of the difference between them. When this is equal to $180°$, all sections of the robot are straight, regardless of relative orientation to gravity. Another failure case under Control 1 was caused by inadequate information from the binary IR touch sensor. Due to placement of the sensor and tilting of the gripper, especially during vertical climbing, the IR sensor would lose contact with the surface although the gripper remained attached. To avoid false positive detection of detachment, we implemented a second check: The robot records the initial orientation of the gripper it wants to detach. It then checks the current orientation of the detaching foot and will only check the touch sensor after the difference between the current and initial orientations is at least $30°$.

III. EXPERIMENTS

A. Locomotion on a flat surface

We first tested the robot on the flat, unconstrained Velcro loop surface, shown in Fig. 7a and the video submission, using Control 1. The robot was placed in the center of the track at the start of each run and completed an average of six continuous flips before it drifted off the Velcro track. The first column of Table I shows the number of successful attachments, successful detachments, total successful flips, and the average time period for a full flip. The robot flipped successfully for 40/40 attempts. In 2/40 attempts, one gripper failed to detach; however, the robot could recover easily by simply detaching and reattach each gripper and trying again.

Fig. 7. Video stills of Flippy robot on a flat, unconstrained track (A) and 2D constrained track (B-H). B) Horizontal to Vertical transition, C) Vertical climbing, D) Vertical to Inverted transition, E)Inverted climbing, F) Inverted to Downward transition, G)Downward to Horizontal transition, H) Climbing and transitioning over approximately 120° and 60° angled surfaces

We also tested the robot climbing vertically, inverted (upside down), downwards, and the transitions between these surfaces in an open box track. The Flippy robot was able to achieve locomotion in all of these orientations; however, since the robot currently cannot steer and is liable to twisting, it was difficult to do a sustained run of more than a few flips, especially while climbing vertically.

TABLE I

SIMPLE CLIMBING RESULTS WITH CONTROL 1 (IR SENSING ONLY)

	Unconstrained	Horizontal	Vertical	Inverted	Down
Attachment	40	13	34	13	14
Detachment	38	13	36	13	14
Successful Flips	40/40	13/13	34/39	13/13	14/14
Avg. Period (s)	23.6	23.7	14.5	18.1	16.9

B. Climbing Locomotion in a 2D Track

We decided to constrain the robot to a 2D track, shown in Fig. 7b-h. The track is made of acrylic with a clear sliding front door and has inside dimensions of 592 x 340 x 45 mm. This allowed for 6-7 flips on the long sides and 1-4 flips (depending on orientation) on the short side, not including transitions. For some tests, the track was flipped 90°, so Flippy could do longer runs on a vertical or downwards track.

The remaining experiments shown in Table I were done inside the track. Vertical climbing is the most difficult for the robot, thus we did additional testing in this mode for a total of 34/39 successful flips. All other locomotion modes had no failures in 13-14 flips. Both early and late detection of detachment by the IR sensor was common, especially in vertical climbing where early detection occurred in 92% of flips, due to tilting of the gripper and the placement of the IR sensor. However, these errors did not effect the robot's ability to flip, demonstrating the robustness of the design.

During these tests, the Flippy robot also attempted to transition between surfaces, but had limited success (0/6 attempts on horizontal to vertical, 2/7 attempts on vertical to inverted, 3/3 attempts on inverted to downward, and 3/5 attempts on downward to horizontal). While Flippy was always able to attach successfully to the new surface, it frequently had trouble detaching, due to the limited touch sensor data and lack of sensory input on its current bending state. Often, the robot would complete the first part of the transition to the new surface, but, on the following flip, would detect the old surface and reattach, resulting in a loop of attaching and reattaching, sometimes requiring human intervention to proceed. Thus we decided to add sensing capacity to the control algorithm, through use of the IMU, resulting in Control 2 (Fig. 6).

C. Climbing in a 2D track with IMU Sensing

With Control 2, the robot was able to complete all four right angle interior transitions as shown in the video submission and in Fig. 7e-g. Table II shows the results from the transition experiments, where H is short for Horizontal, V for Vertical, I for Inverted and D for Downwards. A transition is considered successful if the robot is able to attach to the new surface, detach from the old surface, and then continue to flip along the new surface. The rate of success for all transitions improved significantly from Control 1. The robot was also able to recover from difficult transitions, for example in Fig. 7f, where it was unable to get a good attachment, but was still able to continue to flip downwards.

TABLE II

TRANSITIONS WITH CONTROL 2 (IMU SENSING)

	H to V	V to I	I to D	D to H
Attachment	17	13	15	16
Detachment	17	13	15	16
Continued Locomotion	9	13	15	13
Successful Transitions	9/17	13/13	15/16	13/16

Horizontal to vertical (H to V) transitions remain the most difficult and are affected by the starting position of the robot, which was varied randomly during the trials. The most common errors occurred when the robot attempted to transition far from the vertical wall, as this resulted in lower attachment points. The lower the attachment point, the less space the robot will have on the subsequent flip, sometimes resulting in failure. These errors should be eliminated with improved sensing, as the gripper often made contact much earlier than detected by the touch sensor. Other errors included minor control problems, which may be fixed by using the completely bent position as another threshold. Use of bend sensors, although liable to wear, might also simplify the control, as they depend only on the bending angle and not on the orientation of the robot relative to gravity.

A small number of errors occurred in the other transition experiments. Three were due to attaching too close to the corner on the downwards to horizontal (D to H) transition, though this was improved after recalibration of the touch sensor. One inverted to downwards (I to D) transition also failed to attach, due to the sensors detecting the surface before the corkscrew gripper could fully reach and attach. Thus most of our errors were due to inadequate touch sensing. Because the touch sensors were used as a digital switch, with only one threshold for both attaching and detaching, neither attaching nor detaching could be completely accurate. In future versions of the robot, we plan to improve sensing on the robot gripper by adding at least one additional sensor to account for orientation and by connecting the sensors to an analog input. This should allow for slightly more complex control and improved reliability.

Finally, in Fig. 7h and the attached video, we show that the Flippy robot is capable of transitioning surfaces held at angles other than 90°. This could be important for applications such as search and rescue where debris and other objects may be at odd angles. Here Flippy successfully transitioned twice over an approximately 120° angle and once over a 60° transition. The robot was able to complete these transitions on a thin, flexible ramp, demonstrating the possibility of traversing on unstable surfaces. More testing, however, will be needed to ensure reliability in these transitions.

IV. CONCLUSIONS AND FUTURE WORK

In this paper, we demonstrate the potential of a flipping robot with a compliant body to autonomously climb and transition between planes with simple sensing (a binary touch sensor and IMU), and a basic control algorithm. The robot's small size and on-board power and control are a good fit for inspecting cramped, complex spaces such as pipes or ducts, or performing swarm self-assembly. Though the robot's corkscrew gripper is designed for surfaces covered in Velcro loops, this may be swapped out for different applications.

While the Flippy robot successfully navigated a number of inner transitions, reliability can be further improved with added sensing capacity. Other future improvements include increasing the robot's ability to traverse a large variety of transitions and adding steering. For example, extending the width of the stiff sections would give the robot added reach to complete external transitions or climb over obstacles. This would also have the benefit of increasing the step size and achieving faster movement, though any modifications to geometry should be done with care to minimize the moment arm and necessary gripping force of the robot. We can implement steering in the robot by replacing the two opposing cables with three triangulated cables. This should allow us to move in 3D in a similar manner to robots such as the Treebot [15], which uses triangulated springs.

More generally, Flippy demonstrates the potential of compliant materials in climbing robots, not just those with flipping gaits. The soft joints allow similar capacities as joints with rigid components, such as transitioning between planes, often with less complexity. Additional gaits, such as an inchworm gait could be implemented with the Flippy robot body, or with new compliant designs. Soft materials offer added versatility and a large, open design space which has been mostly unexplored in climbing robots.

REFERENCES

[1] B. Chu, K. Jung, C.-S. Han, and D. Hong, "A survey of climbing robots: Locomotion and adhesion," *International Journal of Precision Engineering and Manufacturing*, vol. 11, no. 4, pp. 633–647, aug 2010.

[2] B. He, Z. Wang, M. Li, K. Wang, R. Shen, and S. Hu, "Wet Adhesion Inspired Bionic Climbing Robot," *IEEE/ASME Transactions on Mechatronics*, vol. 19, no. 1, pp. 312–320, feb 2014.

[3] R. Chen, R. Liu, and H. Shen, "Design of a double-tracked wall climbing robot based on electrostatic adhesion mechanism," in *2013 IEEE Workshop on Advanced Robotics and its Social Impacts*. IEEE, nov 2013, pp. 212–217.

[4] H. Prahlad, R. Pelrine, S. Stanford, J. Marlow, and R. Kornbluh, "Electroadhesive robotswall climbing robots enabled by a novel, robust, and electrically controllable adhesion technology," in *2008 IEEE International Conference on Robotics and Automation*. IEEE, may 2008, pp. 3028–3033.

[5] B. Kennedy, A. Okon, H. Aghazarian, M. Badescu, X. Bao, Y. BarCohen, Z. Chang, B. E. Dabiri, M. Garrett, L. Magnone, and S. Sherrit, "Lemur IIb: a robotic system for steep terrain access," *Industrial Robot: An International Journal*, vol. 33, no. 4, pp. 265–269, jul 2006.

[6] E. W. Hawkes, D. L. Christensen, and M. R. Cutkosky, "Vertical dry adhesive climbing with a 100 bodyweight payload," in *2015 IEEE International Conference on Robotics and Automation (ICRA)*. IEEE, may 2015, pp. 3762–3769.

[7] D. Santos, B. Heyneman, S. Kim, N. Esparza, and M. R. Cutkosky, "Gecko-inspired climbing behaviors on vertical and overhanging surfaces," in *2008 IEEE International Conference on Robotics and Automation*. IEEE, may 2008, pp. 1125–1131.

[8] A. Asbeck, M. Cutkosky, and W. Provancher, "SpinybotII: climbing hard walls with compliant microspines," *ICAR '05. Proceedings., 12th International Conference on Advanced Robotics, 2005.*, pp. 601–606, 2005.

[9] Y. Liu, S. Sun, X. Wu, and T. Mei, "A Wheeled Wall-Climbing Robot with Bio-Inspired Spine Mechanisms," *Journal of Bionic Engineering*, vol. 12, no. 1, pp. 17–28, jan 2015.

[10] M. P. Murphy, C. Kute, Y. Mengüç, and M. Sitti, "Waalbot II: Adhesion Recovery and Improved Performance of a Climbing Robot using Fibrillar Adhesives," *The International Journal of Robotics Research*, vol. 30, no. 1, pp. 118–133, jan 2011.

[11] P. Schoeneich, F. Rochat, O. T.-D. Nguyen, R. Moser, and F. Mondada, "TRIPILLAR: a miniature magnetic caterpillar climbing robot with plane transition ability," *Robotica*, vol. 29, no. 07, pp. 1075–1081, apr 2011.

[12] T. Seo and M. Sitti, "Tank-Like Module-Based Climbing Robot Using Passive Compliant Joints," *IEEE/ASME Transactions on Mechatronics*, vol. 18, no. 1, pp. 397–408, feb 2013.

[13] R. L. Tummala, R. Mukherjee, N. Xi, D. Aslam, H. Dulimarta, J. Xiao, M. Minor, and G. Dang, "Climbing the Walls," *IEEE Robotics & Automation Magazine*, vol. 9, no. 4, pp. 10–19, 2002.

[14] Y. Guan, H. Zhu, W. Wu, X. Zhou, L. Jiang, C. Cai, L. Zhang, and H. Zhang, "A Modular Biped Wall-Climbing Robot With High Mobility and Manipulating Function," *IEEE/ASME Transactions on Mechatronics*, vol. 18, no. 6, pp. 1787–1798, dec 2013.

[15] T. L. Lam and Y. Xu, "A flexible tree climbing robot: Treebot - design and implementation," in *2011 IEEE International Conference on Robotics and Automation*. IEEE, may 2011, pp. 5849–5854.

[16] A. Dollar and R. Howe, "A robust compliant grasper via shape deposition manufacturing," *IEEE/ASME Transactions on Mechatronics*, vol. 11, no. 2, pp. 154–161, apr 2006.

[17] J. Gafford, Y. Ding, A. Harris, T. McKenna, P. Polygerinos, D. Holland, A. Moser, and C. Walsh, "Shape Deposition Manufacturing of a Soft, Atraumatic, Deployable Surgical Grasper1," *Journal of Medical Devices*, vol. 8, no. 3, p. 030927, jul 2014.

[18] H.-T. Lin, G. G. Leisk, and B. Trimmer, "GoQBot: a caterpillar-inspired soft-bodied rolling robot," *Bioinspiration & Biomimetics*, vol. 6, no. 2, p. 026007, jun 2011.

[19] R. Full, K. Earls, M. Wong, and R. Caldwell, "Locomotion like a wheel?" *Nature*, vol. 365, no. 6446, pp. 495–495, oct 1993.

[20] J. W. Romanishin, K. Gilpin, S. Claici, and D. Rus, "3D M-Blocks: Self-reconfiguring robots capable of locomotion via pivoting in three dimensions," in *2015 IEEE International Conference on Robotics and Automation (ICRA)*. IEEE, may 2015, pp. 1925–1932.

[21] M. Wu, G. Pan, T. Zhang, S. Chen, F. Zhuang, and Z. Yan-zheng, "Design and Optimal Research of a Non-Contact Adjustable Magnetic Adhesion Mechanism for a Wall-Climbing Welding Robot," *International Journal of Advanced Robotic Systems*, vol. 10, no. 1, p. 63, jan 2013.

[22] M. J. Spenko, G. C. Haynes, J. A. Saunders, M. R. Cutkosky, A. A. Rizzi, R. J. Full, and D. E. Koditschek, "Biologically inspired climbing with a hexapedal robot," *Journal of Field Robotics*, vol. 25, no. 4-5, pp. 223–242, apr 2008.

[23] A. Parness, M. Frost, N. Thatte, J. P. King, K. Witkoe, M. Nevarez, M. Garrett, H. Aghazarian, and B. Kennedy, "Gravity-independent Rock-climbing Robot and a Sample Acquisition Tool with Microspine Grippers," *Journal of Field Robotics*, vol. 30, no. 6, pp. 897–915, nov 2013.